

1 **A highly polymorphic effector protein promotes fungal virulence through suppression**
2 **of plant-associated Actinobacteria**

3

4 Nick C. Snelders^{1,2,#}, Jordi C. Boshoven^{3,#}, Yin Song^{3,4,\$} Natalie Schmitz^{1,\$}, Gabriel L.
5 Fiorin^{3,\$}, Hanna Rovenich¹, Grady C.M. van den Berg³, David E. Torres^{2,3}, Luigi Faino^{3,5},
6 Michael F. Seidl², Bart P.H.J. Thomma^{1,3,*}

7

8 ¹ University of Cologne, Institute for Plant Sciences, Cluster of Excellence on Plant Sciences
9 (CEPLAS), 50674 Cologne, Germany;

10 ² University of Utrecht, Theoretical Biology and Bioinformatics Group, Department of
11 Biology, 3584CH Utrecht, The Netherlands;

12 ³ Wageningen University and Research, Laboratory of Phytopathology, Droevendaalsesteeg 1,
13 6708PB Wageningen, The Netherlands;

14 ⁴ State Key Laboratory of Crop Stress Biology for Arid Areas and College of Agronomy,
15 Northwest A&F University, Yangling 712100, Shaanxi, China.

16 ⁵ Sapienza University of Rome, Department of Ambiental Biology, 00185 Rome, Italy.

17

18 # These authors contributed equally

19 \$ These authors contributed equally

20 * To whom correspondence should be addressed. E-mail: bthomma@uni-koeln.de

21

22

23 Total word count: 5653

24 Word count Introduction: 904

25 Word count Materials and Methods: 1722

26 Word count Results: 1935

27 Word count Discussion: 950

28 Word count Acknowledgements: 142

29 Number of Figures: 6

30 **ABSTRACT**

31 Plant pathogens secrete effector proteins to support host colonization through a wide range of
32 molecular mechanisms, while plant immune systems evolved receptors to recognize effectors
33 or their activities to mount immune responses to halt pathogens. Importantly, plants do not act
34 as single organisms, but rather as holobionts that actively shape their microbiota as a
35 determinant of health, and may thus be targeted by pathogen effectors as such. The soil-borne
36 fungal pathogen *Verticillium dahliae* was recently demonstrated to exploit the VdAve1 effector
37 to manipulate the host microbiota to promote vascular wilt disease in absence of the
38 corresponding immune receptor Ve1. We now identified a multiallelic *V. dahliae* gene
39 displaying ~65% sequence similarity to *VdAve1*, named *VdAve1-like* (*VdAve1L*). Interestingly,
40 *VdAve1L* shows extreme sequence variation, including alleles that encode dysfunctional
41 proteins, indicative of selection pressure to overcome host recognition. We show that the
42 orphan cell surface receptor Ve2, encoded at the *Ve1* locus, does not recognize VdAve1L.
43 Furthermore, we show that the full-length variant VdAve1L2 possesses antimicrobial activity,
44 like VdAve1, yet with a divergent activity spectrum. Altogether, VdAve1L2 is exploited by *V.*
45 *dahliae* to mediate tomato colonization through the direct suppression of antagonistic
46 Actinobacteria in the host microbiota. Our findings open up strategies for more targeted
47 biocontrol against microbial plant pathogens.

48

49 Key words: Antimicrobial, avirulence factor, effector, holobiont, immune receptor, microbiota,
50 pathogen

51 INTRODUCTION

52 The plethora of microbes a plant associates with, its so-called microbiota, encompasses a
53 diversity of microbes that establish a spectrum of symbiotic relationships with their host,
54 ranging from commensalistic through endophytic to mutualistic and pathogenic (Hassani *et al.*,
55 2019). To survey their microbiota for potentially pathogenic invaders, plants evolved complex
56 immune systems comprising various types of receptors that betray microbial ingress, for
57 instance through the recognition of microbe-associated molecular patterns (MAMPs) or
58 microbially-secreted effector proteins (Chisholm *et al.*, 2006; Jones & Dangl, 2006; Dodds &
59 Rathjen, 2010; Thomma *et al.*, 2011; Cook *et al.*, 2015). If not recognized, microbial effectors
60 play crucial roles during plant colonization. While they can benefit microbes in many ways,
61 most of the effectors functionally characterized to date have been implicated in deregulation of
62 host immune responses or other processes in host physiology (Rovenich *et al.*, 2014; Cook *et*
63 *al.*, 2015; He *et al.*, 2020; Wang *et al.*, 2022). However, novel effector functions are still
64 discovered. For instance, we recently demonstrated that some effectors are secreted to
65 manipulate plant microbiota compositions to promote host colonization (Snelders *et al.*, 2020,
66 2021, 2022).

67 Effector recognition in plants is mediated by resistance (*R*) genes, typically encoding
68 receptors that reside on the cell surface or in the host cell cytoplasm, that detect effectors or
69 their activities to activate effector-triggered immunity (ETI), often leading to avirulence of the
70 pathogen (Chisholm *et al.*, 2006; Jones & Dangl, 2006; Dodds & Rathjen, 2010; Thomma *et*
71 *al.*, 2011; Cook *et al.*, 2015). Consequently, effectors that are recognized by R proteins are
72 referred to as avirulence factors (Avr)(Li *et al.*, 2020). To evade ETI and restore the ability to
73 colonize their hosts, pathogens are known to inactivate, purge or mutate their avirulence genes,
74 or to evolve novel effectors that suppress ETI (van Kan *et al.*, 1991; Armstrong *et al.*, 2005;

75 Gout *et al.*, 2007; Stergiopoulos *et al.*, 2007; Zhou *et al.*, 2013; Wu *et al.*, 2014; Niu *et al.*,
76 2016; Schmidt *et al.*, 2016; Praz *et al.*, 2017).

77 *Verticillium dahliae* is a soil-borne fungal pathogen that causes vascular wilt disease in
78 hundreds of plant species (Fradin & Thomma, 2006). The presumed asexual fungus generates
79 genomic diversity through extensive chromosomal rearrangements and segmental duplications
80 that gave rise to dynamic so-called lineage-specific (LS) regions, more recently referred to as
81 adaptive genomic regions (AGRs) (Klosterman *et al.*, 2011; de Jonge *et al.*, 2013; Faino *et al.*,
82 2016; Shi-Kunne *et al.*, 2018; Cook *et al.*, 2020). These AGRs display extensive
83 presence/absence variation (PAV) between *V. dahliae* strains, are rich in repeats and
84 transposable elements, and have a distinct chromatin profile (Klosterman *et al.*, 2011; de Jonge
85 *et al.*, 2013; Faino *et al.*, 2016; Cook *et al.*, 2020; Torres *et al.*, 2021). Additionally, AGRs are
86 enriched in *in planta*-induced genes and harbor effector genes that are crucial for disease
87 establishment (de Jonge *et al.*, 2012, 2013; Kombrink *et al.*, 2017). Thus, like other filamentous
88 plant pathogens, *V. dahliae* possesses a compartmentalized genome in which (a)virulence
89 factors locate in regions of increased plasticity when compared with the core genome, an
90 arrangement often referred to as a “two-speed” genome (Raffaele & Kamoun, 2012; Dong *et*
91 *al.*, 2015; Torres *et al.*, 2020). Intriguingly, *V. dahliae* AGRs that are conserved between strains
92 display enhanced sequence conservation when compared with core genomic regions (Depotter
93 *et al.*, 2019), underscoring that accelerated evolution in these regions is predominantly
94 mediated by presence–absence polymorphisms.

95 Only few genetic resistance sources to *V. dahliae* have been identified. In tomato, the
96 *Ve* locus provides resistance against *V. dahliae* and has been introgressed into most commercial
97 tomato cultivars (Schaible *et al.*, 1951; Diwan *et al.*, 1999). The *Ve* locus contains two closely
98 linked genes, *SIVe1* and *SIVe2*, that both encode extracellular leucine-rich repeat receptor-like
99 proteins (eLRR-RLPs), of which only *SIVe1* was confirmed to confer *V. dahliae* resistance

100 (Diwan *et al.*, 1999; Kawchuk *et al.*, 2001; Fradin *et al.*, 2009). Since its deployment in the
101 1950s, resistance-breaking strains appeared that have been assigned to race 2, whereas strains
102 that are contained belong to race 1 (Alexander, 1962). Recently, the single dominant *SIV2* locus
103 was shown to mediate race 2 resistance in *Solanum neorickii* and was introgressed in particular
104 tomato rootstock cultivars (Usami *et al.*, 2017). However, resistance-breaking strains already
105 appeared, forming race 3 (Usami *et al.*, 2017; Chavarro-Carrero *et al.*, 2021). Comparative *V.*
106 *dahliae* population genomics led to the identification of the avirulence factors corresponding
107 to *SIVe* and *SIV2* resistance, namely *VdAve1* and *VdAv2*, respectively (de Jonge *et al.*, 2012;
108 Chavarro-Carrero *et al.*, 2021). Both effector genes are located in AGRs and display PAV
109 between *V. dahliae* strains. While the molecular function of *VdAv2* remains unknown, we
110 demonstrated that *VdAve1* promotes virulence of *V. dahliae* on host plants lacking *SIVe1*
111 through selective antimicrobial activity to manipulate host microbiota compositions. More
112 specifically, we showed that *VdAve1* facilitates *V. dahliae* colonization of tomato and cotton
113 through the direct suppression of associated antagonistic bacteria of the Sphingomonadales
114 order (Snelders *et al.*, 2020). Intriguingly, race 1 strains of *V. dahliae* do not display any allelic
115 variation for *VdAve1*, and only two allelic *VdAv2* variants have been identified among race 2
116 strains that differ by one non-synonymous single nucleotide polymorphism (SNP) and that both
117 activate *Av2*-mediated immunity (Chavarro-Carrero *et al.*, 2021). Hence, to date, *V. dahliae*
118 has exclusively been described to evade ETI through loss of complete avirulence genes, and
119 not through gene inactivation or the evolution of allelic effector variants.

120

121 MATERIALS AND METHODS

122 *Verticillium dahliae* genomics

123 Genome sequence data used in this study was obtained previously (Klosterman *et al.*, 2011; de
124 Jonge *et al.*, 2012, 2013; Faino *et al.*, 2015; Chavarro-Carrero *et al.*, 2021). BLAST searches
125 were performed with BLAST+ version 2.11.0 using standard parameters and the nucleotide
126 sequences of *VdAve1* or each of the *VdAve1L* alleles as query. Strains lacking *VdAve1L* in their
127 genome assemblies were further assessed for the presence of the gene by PCR using the primers
128 listed in Supplementary Table 1. Amplicons obtained from each strain were sequenced for
129 allele determination. Discontinuity in the *VdAve1L3* allele was identified by mapping the
130 genomic paired-end sequences to the *V. dahliae* strain JR2 reference genome using BWA-mem
131 (Li & Durbin, 2009; Faino *et al.*, 2015). The genetic diversity and the population structure of
132 the sequenced *V. dahliae* strains was assessed using the reference sequence alignment-based
133 phylogeny builder REALPHY (version 1.12) (Bertels *et al.*, 2014) and Bowtie2 (version 2.2.6)
134 (Langmead & Salzberg, 2012) to map genomic reads against the *V. dahliae* strain JR2 gapless
135 genome. A maximum likelihood phylogenetic tree was built using RAxML (version 8.2.8)
136 (Stamatakis, 2014).

137 Presence-absence variation (PAV) analysis

138 PAV was identified using whole-genome alignments of 52 *V. dahliae* strains. Paired-end short
139 sequencing reads were mapped to reference *V. dahliae* strain JR2 (Faino *et al.*, 2015) using
140 BWA-mem with default settings (Li & Durbin, 2009). Long-reads were mapped to *V. dahliae*
141 JR2 using minimap2 with default settings (Li, 2018). Using the Picard toolkit
142 (<http://broadinstitute.github.io/picard/>), library artifacts were marked and removed with -
143 *MarkDuplicates* followed by *-SortSam* to sort the reads. Raw read coverage was averaged per
144 100 bp non-overlapping windows using the *-multicov* function of BEDtools (Quinlan & Hall,

145 2010). Then, raw read coverage values were transformed to a binary matrix by applying a cut-
146 off of 10 reads for short-read data; ≥ 10 reads indicate presence (1) and < 10 reads indicate
147 absence (0) of the respective genomic region. In the case of long-read data, a cut-off of 1 read
148 was applied; ≥ 1 reads indicate presence (1) and < 1 reads indicate absence (0). This matrix
149 was further summarized to obtain the total number of presence/absence counts in each 100 bp
150 genomic window within 50 kb upstream and downstream of the *VdAve1L* locus.

151 **SNP rate determination of *V. dahliae* genes**

152 To assess if the *VdAve1L* allele indeed displays an unusual degree of sequence variation, we
153 determined the number of SNPs in the CDS of all genes in the genome of *V. dahliae* strain JR2
154 compared to 41 other strains that we previously sequenced using the Illumina platform (Torres
155 *et al.*, 2021). Next, we normalized the identified number of SNPs based on the length of the
156 corresponding CDS to determine a SNP rate.

157 ***VdAve1L2* gene expression**

158 To determine *in planta* expression of *VdAve1L2*, tomato plants (*Solanum lycopersicum*)
159 cultivar MoneyMaker were inoculated with *V. dahliae* strain DVD-S26 as previously described
160 (Fradin *et al.*, 2009). Stems of five mock and five inoculated plants were harvested at 7, 14 and
161 21 days after inoculation. *In vitro* expression of *VdAve1L2* was assessed in mycelium of *V.*
162 *dahliae* strain DVD-S26 grown for 5 days in triplicate on PDA plates and in soil extract
163 (Snelders *et al.*, 2020). Total RNA of all samples was extracted using the Maxwell76 LEV
164 Plant RNA kit (Promega, Leiden, the Netherlands) and cDNA was synthesized using the M-
165 MLV Reverse Transcriptase (Promega, Leiden, the Netherlands). Real-time PCR was
166 conducted using a C1000 Touch™ Thermal Cycler (Bio-Rad, California, USA) and the qPCR
167 SensiMix kit (BioLine, GC Biotech BV, Alphen aan den Rijn, The Netherlands) using the

168 primers listed in Supplementary Table 1. Real-time PCR conditions were as follows: an initial
169 95°C denaturation step for 10 minutes followed by denaturation for 15 seconds at 95°C,
170 annealing for 60 seconds at 60°C, and extension at 72°C for 40 cycles.

171 **Generation of *V. dahliae* mutants**

172 To generate *VdAve1L2* deletion lines, primers were designed to amplify approximately 1500
173 bp up- and downstream of the *VdAve1L2* CDS (Supplementary Table 1). Both amplicons were
174 used to generate a USER-friendly cloning construct to replace *VdAve1L2* by a hygromycin
175 cassette through homologous recombination (Frandsen *et al.*, 2008). To complement the
176 *VdAve1L2* deletion mutant, a PCR fragment was amplified from genomic DNA containing the
177 complete *VdAve1L2* CDS and approximately 1000 bp up- and downstream sequences
178 (Supplementary Table 1) and cloned into the binary vector pCG (Zhou *et al.*, 2013). To
179 generate the *V. dahliae* DVDS-S26 mutants expressing *VdAve1L2* under control of the *VdAve1*
180 promoter, the coding sequence of *VdAve1L2* was amplified and cloned into pFBT005. *V.*
181 *dahliae* transformations were performed as described previously (Santhanam, 2012).

182 **Disease assays**

183 Inoculation of tomato plants to determine the virulence of the *V. dahliae* was performed as
184 described previously (Fradin *et al.*, 2009). Accumulation of *V. dahliae* biomass in the tomato
185 plants was quantified with real-time PCR on the genomic DNA by targeting the internal
186 transcribed spacer (ITS) region of the ribosomal DNA using the primers listed in
187 Supplementary Table 1. To assess the importance of the suppression of Actinobacteria by
188 *VdAve1L2* for tomato colonization by *V. dahliae*, we germinated tomato MoneyMaker seeds
189 in a sealed beaker on sterile potting soil (Lentse potgrond) supplemented with water-treated
190 tomato root microbiota or vancomycin-treated tomato root microbiota. Vancomycin-treatment

191 of the tomato root microbiota was performed as described previously, with slight modifications
192 (Lee *et al.*, 2021). Briefly, roots with rhizosphere soil were harvested from six-week-old
193 tomato MoneyMaker plants grown on potting soil (Lentse potgrond). The material collected
194 from four plants was pooled and ground to a fine powder in liquid nitrogen using mortar and
195 pestle. Subsequently, the ground material was split and transferred to 300 mL 2.5 mM MES
196 pH 6.0 supplemented with 500 µg/mL vancomycin or water. The suspensions were incubated
197 for 3 hours at 30°C and 120 rpm. Finally, the suspensions were divided in fractions of 50 mL,
198 snap frozen and stored at -20°C until use. Tomato seeds were surface-sterilized by incubation
199 for 5 min in 2% sodium hypochlorite. Next, the surface-sterilized tomato seeds were washed
200 three times using sterile water and transferred to sealed beakers containing 60 grams of
201 sterilized potting soil and 50 mL of the water-treated or vancomycin-treated microbial
202 suspensions. After 14 days, seedlings colonized by the microbial communities were root dipped
203 in spore suspensions of *V. dahliae* strain DVD-S26, a *VdAve1L2* deletion mutant or water
204 (mock) as described previously (Fradin *et al.*, 2009) and transferred to pots containing sterile
205 river sand soaked in Hoagland nutrient solution.

206 ***Agrobacterium tumefaciens*-mediated transient expression in *N. tabacum***

207 *Nicotiana tabacum* cv. Petite Havana SR1 was infiltrated with GV3101 *A. tumefaciens* strains
208 carrying pSOL2092 constructs for expression of *Ve1* or *Ve2* and an *VdAve1*(-like) construct, as
209 described previously (Zhang *et al.*, 2013). Plants were transferred to a climate chamber and
210 incubated at 22°C and 19°C during 16-h day and 8-h night periods, respectively, with 70%
211 relative humidity. Leaves were inspected for HR at 5 dpi.

212 **Protein production, purification and refolding**

213 Heterologous production and purification of VdAve1L2 was performed as described
214 previously for VdAve1 (Snelders *et al.*, 2020).

215 **Oxford Nanopore Technology sequencing**

216 Library preparation of the PCR fragment was performed according to the protocol of Oxford
217 Nanopore, skipping the DNA fragmentation step. The library was loaded on a Nanopore flow
218 cell. The run yielded about 870 high quality long reads with an average length of 3,869 bp with
219 the longest read being ~14 kb. Using Nanocorrect, we used all the obtained reads to correct the
220 50 longest reads, of which 28 were corrected to generate a consensus. Finally, reads were used
221 for BLAST analysis to confirm the presence of *VdAve1L3* fragments at both ends.

222 **Root microbiota analysis**

223 Tomato inoculations were performed as described previously (Fradin *et al.*, 2009). After
224 10 days, plants were carefully uprooted and gently shaken to remove loosely adhering soil from
225 the roots. Next, roots with rhizosphere soil from two tomato plants were pooled to form a single
226 biological replicate. Alternatively, the tomato plants that received the water-treated and
227 vancomycin-treated microbial communities were uprooted 18 days post inoculation with *V.*
228 *dahliae* and a single root system with adhering river sand was collected as a biological control.
229 All samples were flash-frozen in liquid nitrogen and ground using mortar and pestle. Genomic
230 DNA isolation was performed using the DNeasy PowerSoil Kit (Qiagen, Venlo, The
231 Netherlands). Sequence libraries were prepared following amplification of the V4 region of the
232 bacterial 16S rDNA (341F and 785R) and paired ends (300 bp) were sequenced using the
233 MiSeq sequencing platform (Illumina) at Baseclear (Leiden, The Netherlands). Data analyses
234 were performed as described previously (Snelders *et al.*, 2020).

235 **Bacterial isolates**

236 Bacterial strains *B. subtilis* AC95, *S. xylosum*. M3, *P. corrugata* C26 and *Ralstonia* sp. M21
237 were obtained from our in house endophyte culture collection (Snelders *et al.*, 2020). Bacterial
238 strains *Aeromicrobium* sp. (DSM 102283), *C. chitinilytica* (DSM 17922), *F. peucedani* (DSM
239 22180), *J. huperziae* (DSM 46866), *Leifsonia* sp. (DSM 102435) and *N. plantarum* (DSM
240 11054) were obtained from the DSMZ culture collection (Braunschweig, Germany). Bacterial
241 strains *Novosphingobium* sp. A (NCCB 100261), *S. macrogoltabida* (NCCB 95163) and
242 *Sphingobacterium* sp. (NCCB 100093) were obtained from the Westerdijk Fungal Biodiversity
243 Institute (Utrecht, the Netherlands).

244 **Antimicrobial activity assays**

245 *In vitro* antimicrobial activity assays were performed as described previously using 0.2x
246 tryptone soy broth as growth medium for the bacteria (Snelders *et al.*, 2020).

247 ***In vitro* competition assays**

248 Following eleven days of cultivation on PDA, the conidiospores of *V. dahliae* strains DVDS26
249 $\Delta VdAve1L2$, DVD-S26 $\Delta VdAve1L2 + pVdAve1::VdAve1L2$ #1 and DVD-S26 $\Delta VdAve1L2 +$
250 $pVdAve1::VdAve1L2$ #2 were harvested from plate and stored at -80° C at a concentration of
251 4×10^5 spores/mL in low salt TSB (17 g/L tryptone, 3 g/L soy peptone, 0.5 g/L NaCl, 2.5 g/L
252 K₂HPO₄ and 2.5 g/L glucose) supplemented with 10% glycerol until use. Next, bacterial
253 isolates were grown on low salt TSA at 28°C. Single colonies were selected and grown
254 overnight at 28°C while shaking at 150 rpm. Overnight cultures were resuspended to an
255 OD₆₀₀=0.02 in fresh low salt TSB, while the fungal spore suspensions were allowed to thaw at
256 room temperature. Finally, the bacterial and fungal spore suspensions were mixed in 500 µl of
257 low salt TSB to a final concentration of OD₆₀₀=0.01 and 10³ spores/mL, respectively.
258 Following six days of incubation at 22°C, the microbial suspensions were transferred to clear

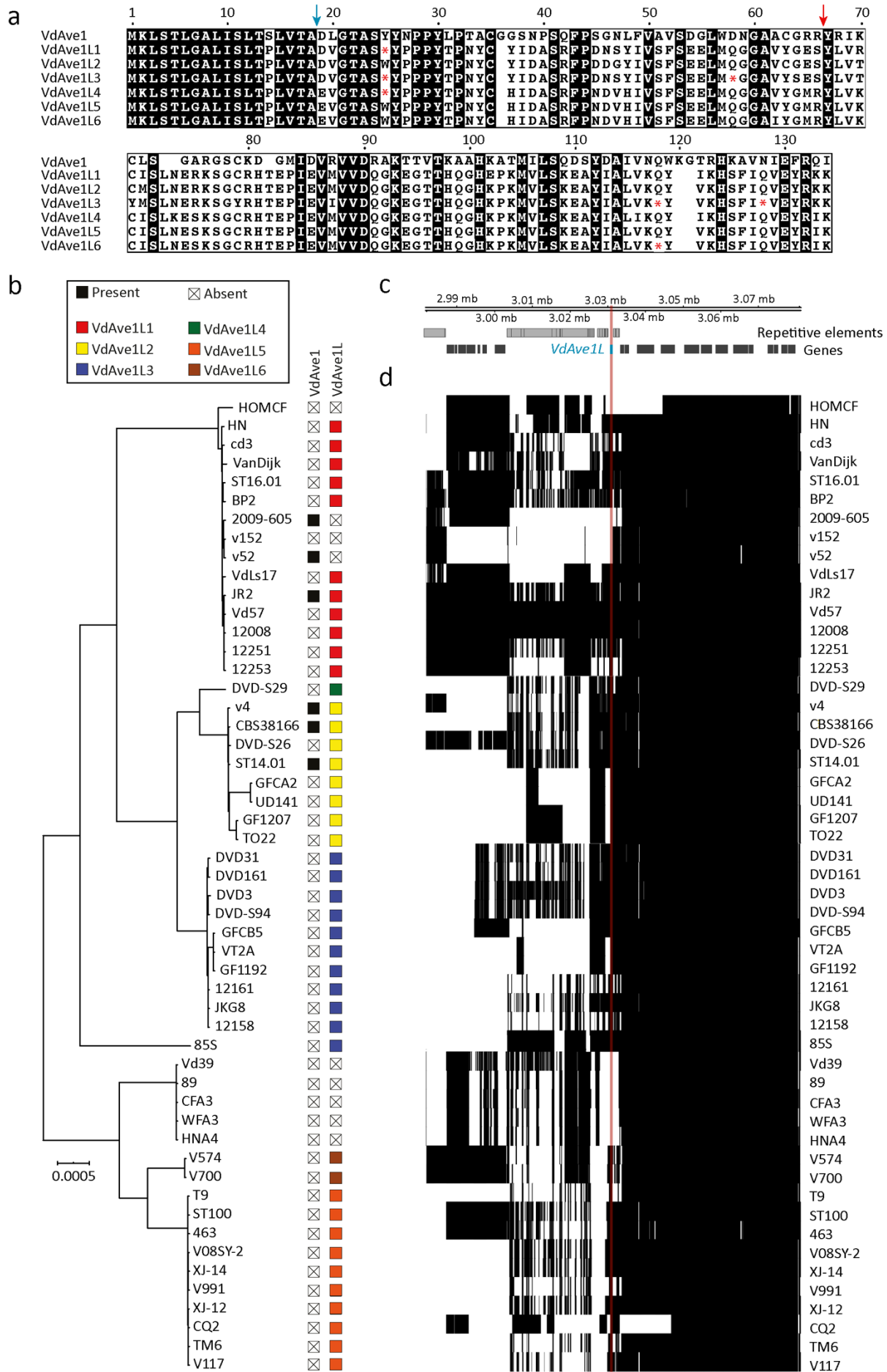
- 259 24-well flat-bottom polystyrene tissue culture plates to allow imaging of fungal growth using
- 260 an SZX10 stereo microscope (Olympus) equipped with a EP50 camera (Olympus).

261 **RESULTS**

262 **Identification of the highly polymorphic *VdAve1*-like gene in an adaptive genomic**
263 **region of *Verticillium dahliae***

264 Using the gapless genome assembly of *V. dahliae* strain JR2 (Faino *et al.*, 2015), a similarity
265 search with the coding sequence (CDS) of *VdAve1* revealed a gene with 67% nucleotide
266 similarity that we further refer to as *VdAve1L* (for *VdAve1*-like). However, while *VdAve1*
267 encodes a 134 amino acid protein (de Jonge *et al.*, 2012), *VdAve1L* only encodes a 24 amino
268 acid protein due to a premature stop codon (Fig. 1a). Searches in the genomes of 51 additional
269 *V. dahliae* isolates (Klosterman *et al.*, 2011; de Jonge *et al.*, 2012; Faino *et al.*, 2015; Chavarro-
270 Carrero *et al.*, 2021) identified the gene in 42 isolates (Fig. 1a,b; Supplementary Fig. 1), albeit
271 with considerable allelic variation. In total we identified six allelic variants (*VdAve1L1* to
272 *VdAve1L6*) that share 93-99% sequence similarity (Fig. 1a,b). Like *VdAve1L1*, also *VdAve1L3*
273 and *VdAve1L4* encode truncated 24 amino acid proteins (Fig. 1a). In contrast, and similar to
274 *VdAve1*, *VdAve1L2* and *VdAve1L5* encode 134 amino acid proteins including an 18 amino acid
275 N-terminal signal peptide (Fig. 1a). Finally, *VdAve1L6* only differs by one amino acid when
276 compared with *VdAve1L5* and is truncated after 120 amino acids (Fig. 1a).

277



279 **Figure 1. *Verticillium dahliae* strains carry a multiallelic *VdAve1*-like gene. (a)** Protein
280 sequence alignment of the identified *VdAve1L* proteins and *VdAve1*. Red asterisks (*) indicate
281 stop codons in the *VdAve1L* alleles. The blue arrow indicates the predicted signal peptide
282 cleavage site, and the red arrow indicates the site where discontinuity is observed in *VdAve1L3*.
283 **(b)** Phylogenetic tree of sequenced *V. dahliae* strains and the presence-absence variation of
284 *VdAve1* and *VdAve1L* alleles in the corresponding genomes. **(c-d)** *VdAve1L* is located in an
285 adaptive genomic region of the *V. dahliae* genome. The matrix displays the presence-absence
286 (black/white) variation in 100 bp non-overlapping windows in the genomic region surrounding
287 *VdAve1L*. The upper panel displays the annotated genes and repetitive elements identified in
288 this genomic region, indicated in black and grey, respectively.

289 Genome assemblies consistently assigned sections of *VdAve1L3* on separate contigs,
290 suggesting discontinuity of this allele. (Supplementary Fig. 2a), which was further supported
291 by PCR analysis on strains DVD-3, DVD-31, DVD-S94 and DVD-161 (Supplementary Fig.
292 2b). To investigate whether the discontinuity is caused by a chromosomal rearrangement or
293 transposable element insertion, we performed the PCR on strain DVD-3 with prolonged
294 elongation time, yielding an amplicon of ~7 kb (Supplementary Fig. 2c). Subsequent sequence
295 analysis revealed that *VdAve1L3* is interrupted by a long terminal repeat retrotransposon
296 classified as VdLTRE3 (Faino *et al.*, 2016).

297 As expected based on the observed PAV among some *V. dahliae* strains (Fig. 1b),
298 *VdAve1L* is localized in an AGR (Fig 1c,d) (Cook *et al.*, 2020). However, the allelic variation
299 of *VdAve1L* is unexpected given the previously observed commonly increased sequence
300 conservation of AGR sequences that are shared among *V. dahliae* strains (Depotter *et al.*,
301 2019). Intriguingly, further analysis revealed that *VdAve1L* displays the highest SNP rate of all
302 genes in the *V. dahliae* genome (Supplementary Fig. 3), and that all of the identified SNPs, 30
303 in total (Supplementary Fig. 4), cause protein sequence variation. Thus, *VdAve1L* is a highly
304 polymorphic gene that displays accelerated evolution by PAV, transposon-mediated sequence
305 disruption, and sequence variation.

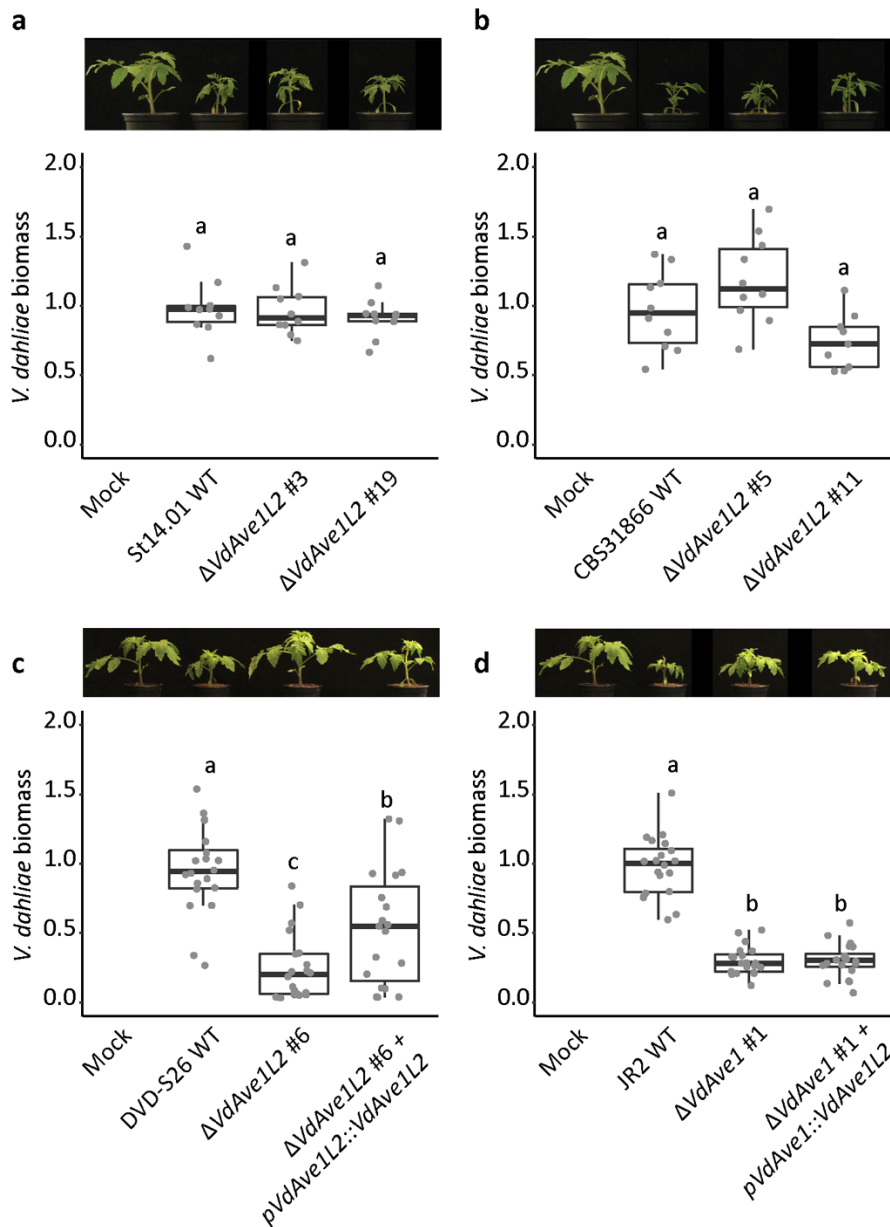
306 **VdAve1L proteins are not recognized by SIVe2**

307 The extreme sequence variation of VdAve1L is likely the result of selection pressure to
308 overcome recognition by a plant immune receptor. The only *R* gene known to confer resistance
309 to *V. dahliae* is tomato *SIVe1* (Kawchuk *et al.*, 2001; Fradin *et al.*, 2009), which resides in the
310 *Ve* locus together with *SIVe2* that similarly encodes a receptor-like protein (Fradin *et al.*, 2009).
311 *SIVe2* is expressed similarly as *SIVe1*, yet the encoded receptor does not recognize VdAve1
312 and its function remains unknown (Fradin *et al.*, 2009; de Jonge *et al.*, 2012). Thus, we tested
313 if SIVe2 can recognize a current or predicted ancestral VdAve1L variant. To this end, we
314 reversed disruptive mutations in *VdAve1L1*, *VdAve1L3* and *VdAve1L4* by replacing premature
315 stop codons with corresponding codons in *VdAve1L2* and *VdAve1L5* to yield the derivatives
316 *VdAve1L1**, *VdAve1L3** and *VdAve1L4** (Fig. 2a,b). Similarly, we replaced stop codons in
317 *VdAve1L3** and removed the retrotransposon (Fig. 2a,b). Additionally, based on an alignment
318 consensus sequence we constructed the predicted common *VdAve1L* ancestor *VdAve1L***
319 (Fig.2a,b). Subsequently, we co-expressed the various genes with *SIVe2* in *Nicotiana tabacum*,
320 and with *SIVe1* as a negative control, but no hypersensitive response (HR) could be observed
321 except upon co-expression of *SIVe1* (Fig. 2c). Consequently, it is unlikely that SIVe2
322 recognized VdAve1L and drove its diversification.

341 **VdAve1L2 is a virulence factor that functionally diverged from VdAve1**

342 Only the alleles *VdAve1L2* and *VdAve1L5* encode full length proteins (Fig. 1), yet none of the
343 strains that encodes *VdAve1L5* is pathogenic on tomato (Li, 2019). To determine if
344 *VdAve1L2*, like *VdAve1*, contributes to virulence on tomato, we assessed its expression in *V.*
345 *dahliae* race 2 strain DVD-S26 during host colonization, showing clear expression *in planta*
346 (Supplementary Fig. 5). Interestingly, while we previously also detected expression of *VdAve1*
347 during cultivation *in vitro* on PDA and in soil extract (Snelders *et al.*, 2020), we did not detect
348 *VdAve1L2* expression under these conditions (Supplementary Fig. 5).

349 To determine the importance of *VdAve1L2* for tomato colonization, we generated
350 deletion mutants in the race 2 strain DVD-S26 and in the race 1 strains ST14.01 and CBS38166
351 (Supplementary Fig. 6). Inoculation of tomato plants with the deletion mutants of the race 1
352 strains revealed no virulence contribution of *VdAve1L2* (Fig 3a,b). Strikingly, however, we
353 detected strongly compromised tomato colonization of the *VdAve1L2* deletion mutant in strain
354 DVD-S26 (Fig 3c), which was restored in a complementation mutant (Fig. 3c). Thus,
355 *VdAve1L2* contributes to *V. dahliae* virulence on tomato in the absence of *VdAve1*. To address
356 the hypothesis that *VdAve1* and *VdAve1L2* are functionally redundant, we introduced
357 *VdAve1L2* under control of the *VdAve1* promoter in a *VdAve1* deletion mutant of the JR2 strain
358 and tested its virulence on tomato, yet *VdAve1L2* failed to restore the virulence penalty of
359 *VdAve1* deletion. Collectively, our data suggest that *VdAve1* and *VdAve1L2* have functionally
360 diverged.



361

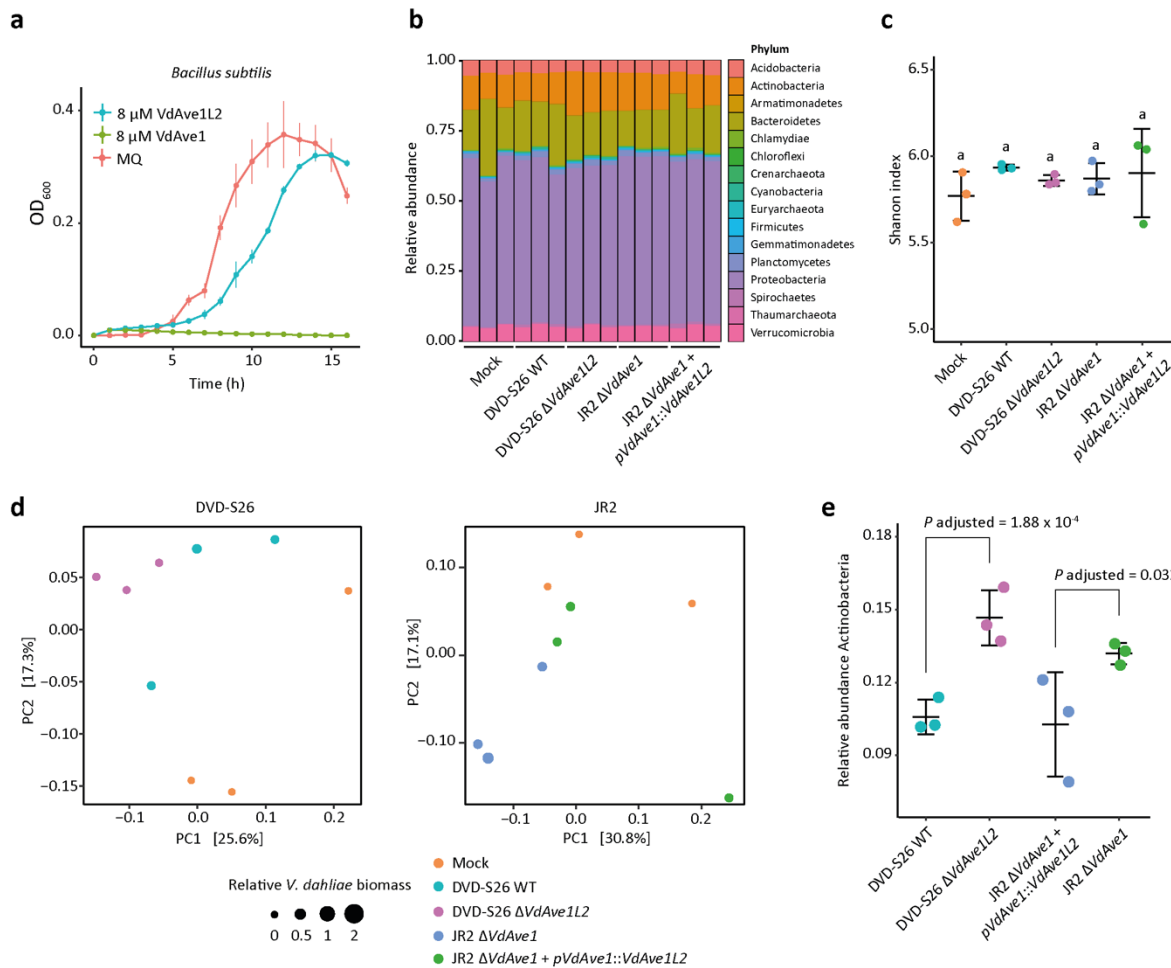
362 **Figure 3. VdAve1L2 is a virulence factor of *V. dahliae* that functionally diverged from**
 363 **VdAve1. (a-b) VdAve1L2 does not contribute to virulence of *V. dahliae* race 1 strains St14.01**
 364 **(a) and CBS31866 (b) on tomato. Photos display representative stunting symptoms of tomato**
 365 **plants 14 days post inoculation with wild-type *V. dahliae* strains and the corresponding**
 366 ***VdAve1L2* deletion mutants. *V. dahliae* biomass in tomato stems was quantified by real-time**
 367 **PCR. Letters represent non-significant biomass differences (one-way ANOVA and Tukey's**
 368 **post hoc test; p<0.05; N=10). (c-d) VdAve1L2 contributes to virulence of *V. dahliae* race 2**
 369 **strain DVD-S26 on tomato (c) but fails to restore the virulence that is lost by *V. dahliae* race 1**
 370 **strain JR2 upon deletion of *VdAve1*. (d) Photos display representative stunting phenotypes of**
 371 **tomato plants 14 days post inoculation with the wild-type *V. dahliae* strains, the corresponding**
 372 ***VdAve1L2* or *VdAve1* deletion mutants, and the mutants expressing *VdAve1L2* under control of**
 373 **its native or *VdAve1* promoter. *V. dahliae* biomass in tomato stems was quantified by real-time**
 374 **PCR. Letters represent non-significant biomass differences (one-way ANOVA and Tukey's**
 375 **post hoc test; p<0.05; N≥17).**

376 **VdAve1L2 promotes *V. dahliae* virulence through suppression of Actinobacteria**

377 While most effector proteins functionally characterized to date act in manipulation of host
378 physiology, we recently showed that VdAve1 is an antibacterial effector protein that is secreted
379 by *V. dahliae* to suppress microbial antagonists in the microbiomes of its hosts (Snelders *et al.*,
380 2020). Thus, we hypothesized that VdAve1L2 may similarly exert antibacterial activity. *In*
381 *vitro* assays previously revealed a strong activity of VdAve1 on the Gram positive bacterium
382 *Bacillus subtilis* (Snelders *et al.*, 2020). Interestingly, VdAve1L2 affected *B. subtilis* growth as
383 well, albeit markedly less effectively (Fig. 4a). Furthermore, similar to VdAve1 (Snelders *et*
384 *al.*, 2020), VdAve1L2 inhibited the growth of plant-associated *Novosphingobium* sp. and
385 *Staphylococcus xylosum*, but not of *Agrobacterium tumefaciens*, *Pseudomonas corrugata* and
386 *Ralstonia* sp.. However, in contrast to VdAve1, VdAve1L2 did not inhibit growth of
387 *Sphingobacterium* sp. (Supplementary Fig. 7). Collectively, we conclude that VdAve1L2 is an
388 antibacterial effector with a diverged activity spectrum when compared with VdAve1.

389 To determine if VdAve1L2 secretion by *V. dahliae* impacts host microbiota, we
390 performed bacterial community analysis based on 16S ribosomal DNA profiling on tomato
391 roots colonized by *V. dahliae* strain DVD-S26 and the *VdAve1L2* deletion mutant. Furthermore,
392 the *VdAve1* deletion mutant of *V. dahliae* strain JR2 and the corresponding transformant
393 expressing *VdAve1L2* were included. In correspondence with previous observations (Snelders
394 *et al.*, 2020), colonization by *V. dahliae* did not dramatically impact the overall composition of
395 bacterial phyla in tomato root microbiota, and also not their α -diversities (Fig. 4b,c).
396 Importantly, however, a principal coordinate analysis based on Bray-Curtis dissimilarities (β -
397 diversity) revealed separation of the bacterial communities based on *V. dahliae* genotype (Fig.
398 4d), suggesting that secretion of VdAve1L2 impacts root microbiota compositions. Based on
399 pairwise comparisons between the abundances of the bacterial phyla detected in the microbiota
400 in the presence and the absence of VdAve1L2, we identified Actinobacteria as the sole phylum

401 that was significantly suppressed in the microbiota colonized by *V. dahliae* strains secreting
 402 VdAve1L2 (Fig. 4e).



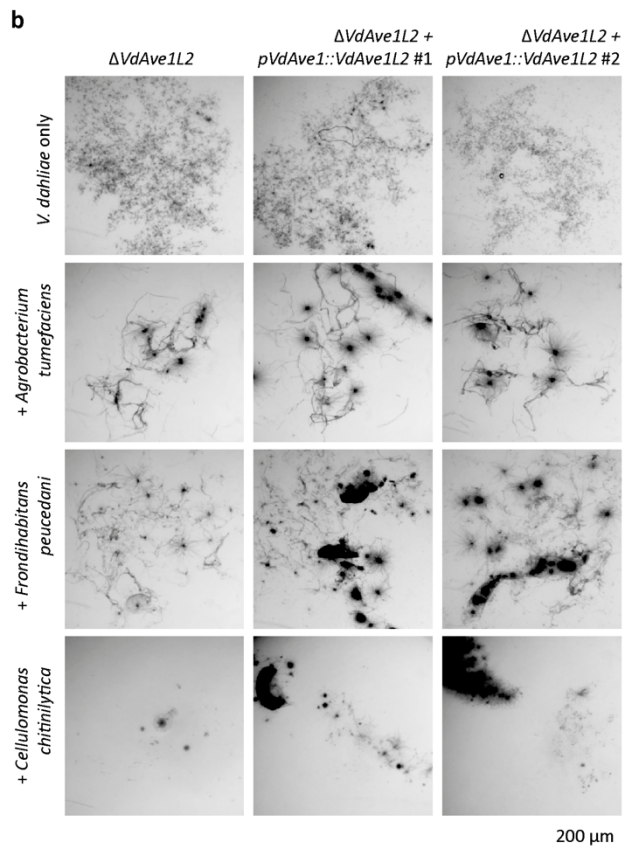
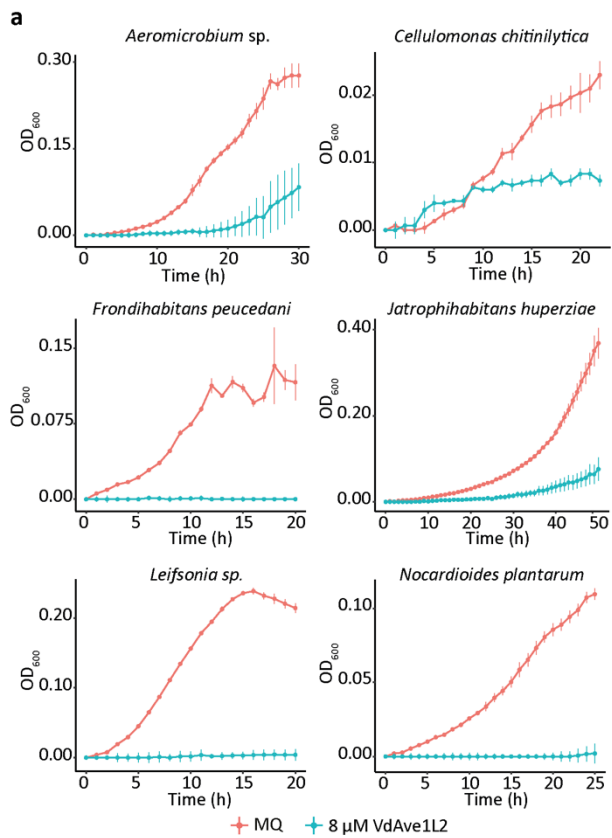
403

404 **Figure 4. VdAve1L2 impacts Actinobacteria in the tomato root microbiota.** (a) VdAve1L2
 405 is an antibacterial effector protein. *In vitro* growth of *Bacillus subtilis* is inhibited by
 406 VdAve1L2. The previously characterized antibacterial effector VdAve1 (Snelders *et al.*, 2020)
 407 was included as positive control for bacterial growth inhibition and displays a differential
 408 activity compared to VdAve1L2. Ultrapure water (MQ) was included as negative control.
 409 Graph displays the average OD₆₀₀ of three biological replicates ± SD. (b) Relative abundance
 410 of bacterial phyla in tomato root microbiota ten days after inoculation with wild-type *V. dahliae*
 411 strain DVD-S26, the corresponding DVD-S26 *VdAve1L2* deletion mutant, a *V. dahliae* strain
 412 JR2 *VdAve1* deletion mutant and the corresponding *VdAve1L2* expression mutant as
 413 determined by 16S ribosomal DNA profiling. (c) *V. dahliae* colonization does not impact α-
 414 diversity of tomato root microbiota. The plot displays the average Shannon index ± SD (one-
 415 way ANOVA and Tukey's post-hoc test; p<0.05; N=3). (d) Principal coordinate analysis based
 416 on Bray-Curtis dissimilarities uncovers separation of root microbiome compositions based on
 417 presence of VdAve1L2. (e) Differential abundance analysis of bacterial phyla reveals a
 418 repression of Actinobacteria in the tomato root microbiota colonized by *V. dahliae* strains that
 419 secrete VdAve1L2 (Wald test, N=3).

420 To test whether the suppression of Actinobacteria is the direct consequence of
421 antimicrobial activity of VdAve1L2, we incubated representatives of three of the most
422 abundant Actinobacterial families, *Nocardioideae*, *Microbacteriaceae* and
423 *Cryptosporangiaceae*, with VdAve1L2 and monitored their growth *in vitro*. Intriguingly, all
424 tested Actinobacteria displayed higher sensitivity to the effector than most of the other bacteria
425 tested thus far (Fig. 5a), suggesting that Actinobacteria are genuine and direct targets of
426 VdAve1L2 *in planta*.

427 Actinobacteria are important players of plant-associated microbial communities, and
428 have repeatedly been assigned roles in disease suppression (Berendsen *et al.*, 2018; Chen *et al.*,
429 2020; Lee *et al.*, 2021). In accordance with their capacity to produce antimicrobial
430 secondary metabolites, suppression of microbial pathogens by Actinobacteria often involves
431 direct antibiosis, although they have also been implicated in the induction of systemic
432 immunity (Conn *et al.*, 2008; Berendsen *et al.*, 2018; van Bergeijk *et al.*, 2020; Lee *et al.*,
433 2021). To test whether *V. dahliae* exploits VdAve1L2 to compete with Actinobacteria, we co-
434 cultivated the *VdAve1L2* deletion mutant of *V. dahliae* strain DVD-S26 with the VdAve1L2-
435 sensitive Actinobacteria *Frondehabtians peucedani* and *Cellulomonas chitinilytica* and the
436 VdAve1L2-insensitive Proteobacterium *Agrobacterium tumefaciens*. Furthermore, we
437 included transformants of the *VdAve1L2* deletion mutant that express *VdAve1L2* under control
438 of the *VdAve1* promoter that is highly active during *in vitro* growth, in contrast to the
439 VdAve1L2 promoter (Supplementary Fig. 5; Supplementary Fig. 8). As anticipated, secretion
440 of VdAve1L2 failed to counter the antagonistic activity of *A. tumefaciens* and did not promote
441 *V. dahliae* growth when confronted with this bacterium (Fig. 5b). However, *V. dahliae* clearly
442 benefited from VdAve1L2 secretion in competition with both Actinobacteria, as it mediated
443 enhanced fungal growth and development of larger colonies (Fig. 5b). Collectively, our

444 findings suggest that *V. dahliae* secretes VdAve1L2 to antagonize Actinobacteria in the host
 445 microbiota.

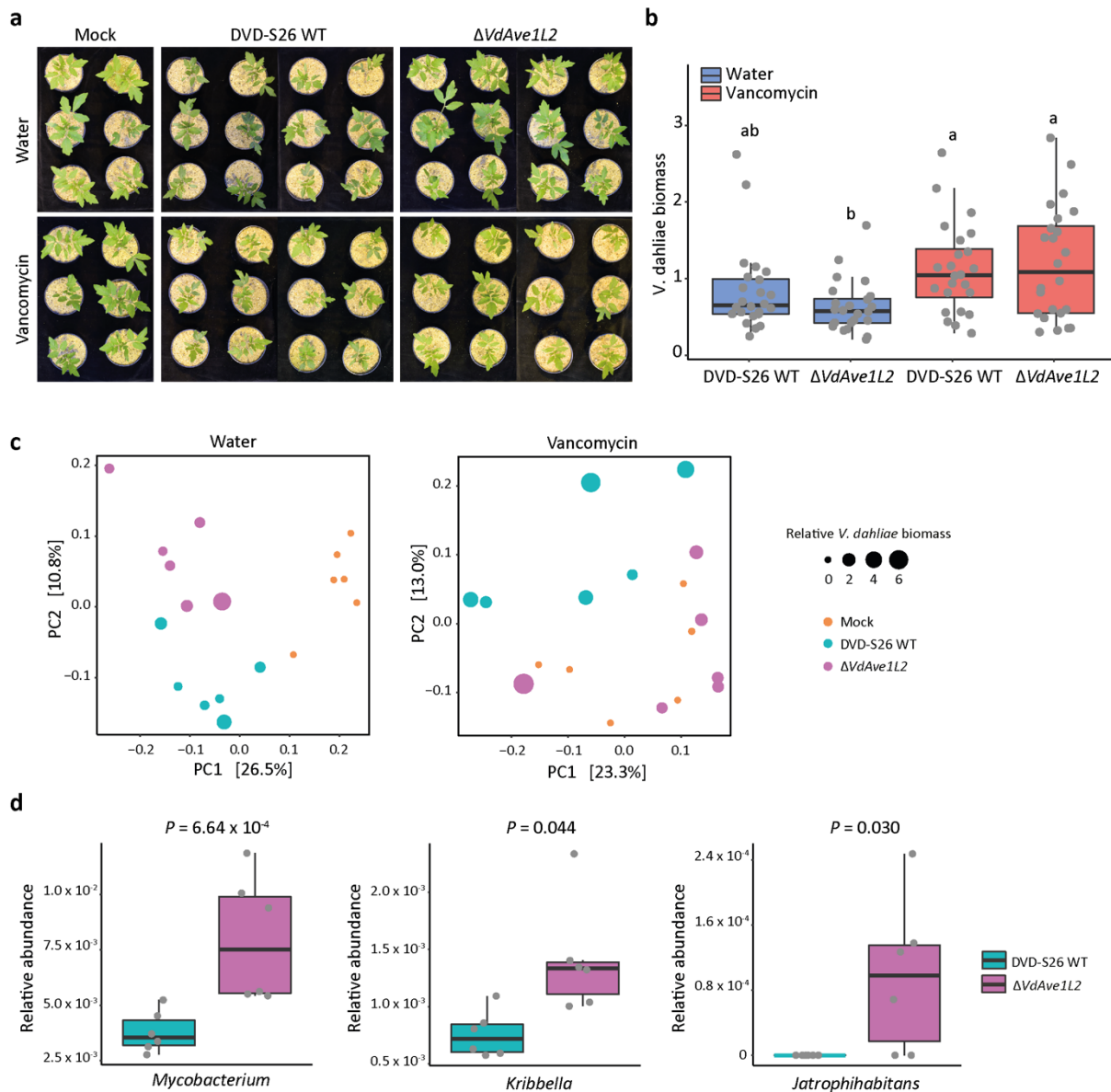


448 **Figure 5. *Verticillium dahliae* VdAve1L2 affects antagonistic Actinobacteria (a)**
449 Actinobacteria are inhibited by VdAve1L2. Graphs display the average OD₆₀₀ of three
450 biological replicates \pm SD. **(b)** VdAve1L2 supports *V. dahliae* growth in the presence of
451 antagonistic Actinobacteria. Representative microscopic pictures displaying the *VdAve1L2*
452 deletion mutant and two mutants expressing *VdAve1L2* under control of the *VdAve1* promoter
453 cultivated for six days in the presence of the *VdAve1L2*-insensitive Proteobacterium
454 *Agrobacterium tumefaciens* and the *VdAve1L2*-sensitive Actinobacteria *Fron dihabtians*
455 *peucedani* and *Cellulomonas chitinilytica*.
456

457 Next, we aimed to determine the importance of the suppression of Actinobacteria by
458 VdAve1L2 for tomato colonization by *V. dahliae*. Following a previously described protocol
459 (Lee *et al.*, 2021), we extracted the root microbiota from tomato plants followed by incubation
460 with the Gram positive bacteria-specific antibiotic vancomycin to affect Actinobacteria.
461 Subsequently, the vancomycin-treated communities and water-treated control communities
462 were allowed to establish on tomato seedlings grown under sterile conditions. Finally, the
463 plants were inoculated with *V. dahliae* strain DVD-S26 and the *VdAve1L2* deletion mutant to
464 determine if manipulation of the Actinobacteria affected *V. dahliae* host colonization and
465 assess the virulence contribution of VdAve1L2. As determined using 16S ribosomal DNA
466 profiling, the tomato plants exposed to the vancomycin-treated microbiota did not harbor a
467 dramatically altered community of bacterial phyla when compared with plants exposed to the
468 water-treated microbiota (Supplementary Fig. 9a). Moreover, the vancomycin treatment did
469 not affect the α -diversity or total abundance of bacteria in the plant microbiota (Supplementary
470 Fig. 9b,c). However, as anticipated, we detected a severe impact of vancomycin treatment on
471 the Actinobacteria community structure (Supplementary Fig. 9d). Moreover, phenotypic
472 assessment revealed markedly increased stunting of tomato plants harboring the vancomycin-
473 treated microbiota when compared with plants containing the water-treated community when
474 inoculated with the *VdAve1L2* deletion mutant, showing disease suppression by Actinobacteria
475 in the water-treated community (Fig. 6a). Quantification of *V. dahliae* biomass in the root
476 microbiomes using real-time PCR confirmed significantly increased colonization by the

477 *VdAve1L2* deletion mutant in the presence of the vancomycin-treated microbiota (Fig. 6b).
478 Importantly, while on plants that were treated with the water-treated community *VdAve1L2*
479 markedly contributes to virulence (Fig. 6a), this virulence contribution is not observed on plants
480 that were treated with the vancomycin-treated community, in line with the hypothesis that the
481 Actinobacteria that are targeted by *VdAve1L2* are no longer present in the host microbiota
482 (Fig. 6a). Accordingly, in contrast to the microbiomes with the water-treated microbial
483 community, principal coordinate analysis based on Bray-Curtis dissimilarities (β -diversity)
484 failed to reveal a clear separation of the root microbiomes with the vancomycin-treated
485 community based on their colonization by the different *V. dahliae* strains or mock treatment
486 (Fig. 6c). Moreover, we only detected a *VdAve1L2*-mediated repression of Actinobacteria
487 genera in plants that received the water-treated communities (Fig. 6d). Likely, treatment with
488 vancomycin limited the abundance of antagonistic Actinobacteria such that interference by
489 *VdAve1L2* is no longer required for optimal *V. dahliae* colonization. In conclusion, our
490 findings suggest that Actinobacteria in the tomato root microbiota antagonize host colonization
491 by *V. dahliae*, and that the fungus exploits *VdAve1L2* in turn to suppress these antagonists and
492 promote disease.

493



494

495 **Figure 6. Treatment of tomato root microbiota with vancomycin diminishes the virulence**
 496 **contribution of VdAve1L2. (a)** Phenotypes of tomato plants harboring vancomycin-treated or
 497 water-treated microbial communities infected by wild-type *V. dahliae* and the *VdAve1L2*
 498 deletion mutant at 19 days post inoculation. **(b)** Relative *V. dahliae* biomass in tomato stem
 499 tissue determined with real-time PCR (one-way ANOVA and Tukey's post-hoc test; $p < 0.05$;
 500 $N = 24$) **(c)** Principal coordinate analysis based on Bray-Curtis dissimilarities uncovers
 501 separation of root microbiota compositions in tomato plants harboring water-treated microbial
 502 communities, but not vancomycin-treated microbial communities colonized by both *V. dahliae*
 503 strains and upon mock treatment. **(d)** Relative abundance of the three Actinobacterial genera
 504 that are depleted from the tomato plants harboring the water-treated microbial community
 505 colonized by *V. dahliae* WT when compared with colonization by the *VdAve1L2* deletion
 506 mutant (Wald test; $N = 6$).

507 DISCUSSION

508 To escape recognition by host immune receptors, microbial plant pathogens rely on the
509 inactivation, loss, or mutation of effectors that become recognized. Unlike many microbial
510 plant pathogens for which allelic effector gene variants escaping recognition have been
511 reported (Armstrong *et al.*, 2005; Wu *et al.*, 2014), *V. dahliae* was only known to evade effector
512 recognition through purging complete virulence genes, particularly of *VdAve1* and *VdAv2* (de
513 Jonge *et al.*, 2012; Chavarro-Carrero *et al.*, 2021). Here, we report the discovery of *VdAve1L*,
514 an effector gene with considerable sequence similarity to *VdAve1*, yet that displays
515 extraordinary allelic variation in the *V. dahliae* population, which most likely results from
516 selection pressure imposed by a plant immune receptor.

517 Functional characterization of the full-length effector variant *VdAve1L2* uncovered
518 that this effector, like its homolog *VdAve1*, exerts antibacterial activity to directly suppress
519 microbial competitors *in planta*. Remarkably, however, *VdAve1L2* is exclusively expressed
520 during plant colonization and, in contrast to *VdAve1*, not expressed *in vitro* or in soil.
521 Moreover, the two effectors display distinct antibacterial activities *in vitro*. Accordingly, we
522 observed that secretion of *VdAve1L2* by the race 2 strain DVD-S26, unlike *VdAve1* secreted
523 by the race 1 strain JR2, impacts the abundance of Actinobacteria and not of Sphingomonadales
524 in tomato. *VdAve1L2* and *VdAve1* thus functionally diverged from each other. So far, the
525 mode of action of *VdAve1* remains unclear and, accordingly, it is unclear how *VdAve1L2*
526 functionally diverged from *VdAve1* to target Actinobacteria rather than Sphingomonadales.

527 Actinobacteria represent a core phylum that is found in virtually any plant grown in any
528 environment. Several Actinobacterial species were shown to fulfill beneficial roles in plant
529 holobionts, such as suppression of plant diseases (Berendsen *et al.*, 2018; Chen *et al.*, 2020;
530 Lee *et al.*, 2021). Additionally, Actinobacteria are keystone taxa that impact and benefit
531 microbial community structures in plants (Carlström *et al.*, 2019; Gómez-Pérez *et al.*, 2022).

532 Considering these beneficial traits, it is not surprising that members of this phylum are targeted
533 by microbial plant pathogens to weaken plant holobionts. Interestingly, the oomycete
534 Arabidopsis pathogen *Albugo candida* was recently reported to deposit several antibacterial
535 effector proteins in the leaf apoplast (Gómez-Pérez *et al.*, 2022). Interestingly, some of these
536 effectors impact growth of Actinobacterial keystone taxa of the Arabidopsis phyllosphere *in*
537 *vitro*, suggesting that the suppression of Actinobacteria in host microbiota might be a strategy
538 adopted by diverse microbial plant pathogens. These findings furthermore support the
539 hypothesis that effector-mediated manipulation of host microbiota communities may be a
540 widely deployed strategy of plant pathogens to support host colonization (Snelders *et al.*,
541 2022).

542 VdAve1 is recognized by the tomato immune receptor SIVe1, encoded by a gene in a
543 locus that also encodes the highly similar orphan receptor SIVe2 (Fradin *et al.*, 2014).
544 Considering the similarity between *VdAve1* and *VdAve1L*, we tested if SIVe2 was able to
545 recognize any of the current *VdAve1L* alleles or their putative progenitors, but none of those
546 evoked a detectable hypersensitive response upon overexpression in combination with SIVe2.
547 However, if recognition took place in tomato, it may equally well have been mediated by any
548 other putative immune receptor encoded in the tomato genome. Perhaps even more likely,
549 recognition may also have occurred in any of the hundreds of other *V. dahliae* hosts.
550 Importantly, Actinobacteria are ubiquitously present in a wide diversity of plants, and thus *V.*
551 *dahliae* is likely to benefit from the antibacterial activity of VdAve1L2 in plant species beyond
552 tomato.

553 We previously showed that *VdAve1* was horizontally acquired from plants, where the
554 abundantly present homologs are generally annotated as plant natriuretic peptides (PNPs) (de
555 Jonge *et al.*, 2012). The fact that some of the sequenced *V. dahliae* isolates carry both *VdAve1*
556 and *VdAve1L* raises the question if both genes have been introduced by two separate horizontal

557 gene transfer (HGT) events, or whether only a single HGT event took place that was followed
558 by gene duplication and divergence. Although we have tried to resolve what scenario is most
559 likely, our (phylogenetic) analyses rendered inconclusive results. Hence, at present the exact
560 relationship between VdAve1 and VdAve1L remains unclear. Nevertheless, with VdAve1L2
561 we here reported the characterization of the fourth *V. dahliae* effector protein that acts in
562 microbiota manipulation (Snelders *et al.*, 2020, 2021), which following VdAve1 (de Jonge *et*
563 *al.*, 2012), is most likely the second microbiota-manipulating effector secreted by *V. dahliae*
564 that is recognized by a plant immune receptor. In light of the view that the microbiota
565 constitutes an extrinsic layer of the plant immune system (Dini-Andreote, 2020), microbiota-
566 manipulating effectors target a critical immune component of the host, and thus constitute a
567 relevant target for surveillance by plants to mediate timely pathogen detection, in a similar
568 fashion as effector proteins that interfere with intrinsic immune components are perceived. As
569 a consequence of recognition, microbial plant pathogens need to mutate, purge or inactivate
570 their microbiota-manipulating effector proteins to escape host recognition, which leads to
571 pathogen races with divergent suites of antimicrobial effectors. A possibility for the more
572 effective use of microbial biocontrol agents could be to base their selection on the genotype of
573 a plant pathogen, for instance by selecting antagonists that are insensitive to the activity of a
574 specific (lineage-specific) effector. Conversely, in case a resistance gene has been described to
575 recognize a microbiota-manipulating effector protein, the application of a strong antagonistic
576 biocontrol agent that is sensitive towards the activity of the corresponding effector can be
577 considered. In this manner, a strong selection pressure is exerted to retain that particular
578 effector gene in the pathogen, which may contribute to enhanced durability of the resistance in
579 turn. In this manner, the further identification and characterization of microbiota-manipulating
580 effectors secreted by microbial plant pathogens may aid in the development of more
581 sophisticated, and perhaps more successful, biocontrol strategies.

582 **ACKNOWLEDGEMENTS**

583 Y.S., G.L.F. and D.E.T. acknowledge PhD fellowships from the China Scholarship Council
584 (CSC), Coordination for the Improvement of Higher Education Personnel (CAPES) from the
585 federal government of Brazil, and the Consejo Nacional de Ciencia y Tecnología de México,
586 respectively. The authors thank Bert Essenstam and Pauline Sanderson (Unifarm) for excellent
587 plant care, as well as José Espejo Valle-Inclan for assistance with the Oxford Nanopore
588 MinION sequencing. B.P.H.J.T acknowledges funding by the Alexander von Humboldt
589 Foundation in the framework of an Alexander von Humboldt Professorship endowed by the
590 German Federal Ministry of Education and Research is furthermore supported by the Deutsche
591 Forschungsgemeinschaft (DFG, German Research Foundation) under Germany's Excellence
592 Strategy – EXC 2048/1 – Project ID: 390686111 and by the Research Council for Earth and
593 Life Science (ALW) of the Netherlands Organization for Scientific Research (NWO). The
594 authors declare no conflict of interest exists.

595

596 **AUTHOR CONTRIBUTIONS**

597 N.C.S., J.C.B., and B.P.H.J.T. conceived the project. N.C.S., J.C.B., Y.S., N.S., G.L.F., H.R.,
598 G.C.M.B, D.E.T., L.F., M.F.S. and B.P.H.J.T designed and performed the experiments. N.C.S.,
599 J.C.B., Y.S., N.S., G.L.F., H.R., G.C.M.B, D.E.T., L.F., M.F.S. and B.P.H.J.T. analyzed the
600 data. N.C.S., J.C.B., G.L.F. and B.P.H.J.T. wrote the manuscript. All authors read and approved
601 the final manuscript.

602 **DATA AVAILABILITY**

603 The 16S profiling data have been deposited in the NCBI GenBank database under BioProject
604 PRJNA742137.

605 **REFERENCES**

- 606 **Alexander LJ. 1962.** Susceptibility of certain *Verticillium*-resistant Tomato varieties to an
607 Ohio isolate of the pathogen. *Phytopathology* **52**: 998-1000 pp.
- 608 **Armstrong MR, Whisson SC, Pritchard L, Bos JIB, Venter E, Avrova AO, Rehmany AP,**
609 **Böhme U, Brooks K, Cherevach I. 2005.** An ancestral oomycete locus contains late blight
610 avirulence gene *Avr3a*, encoding a protein that is recognized in the host cytoplasm.
611 *Proceedings of the National Academy of Sciences* **102**: 7766–7771.
- 612 **Berendsen RL, Vismans G, Yu K, Song Y, de Jonge R, Burgman WP, Burmølle M,**
613 **Herschend J, Bakker PAHM, Pieterse CMJ. 2018.** Disease-induced assemblage of a plant-
614 beneficial bacterial consortium. *The ISME journal* **12**: 1496–1507.
- 615 **van Bergeijk DA, Terlouw BR, Medema MH, van Wezel GP. 2020.** Ecology and genomics
616 of Actinobacteria: new concepts for natural product discovery. *Nature Reviews Microbiology*
617 **18**: 546–558.
- 618 **Bertels F, Silander OK, Pachkov M, Rainey PB, Van Nimwegen E. 2014.** Automated
619 Reconstruction of Whole-Genome Phylogenies from Short-Sequence Reads. *Molecular*
620 *Biology and Evolution* **31**: 1077–1088.
- 621 **Carlström CI, Field CM, Bortfeld-Miller M, Müller B, Sunagawa S, Vorholt JA. 2019.**
622 Synthetic microbiota reveal priority effects and keystone strains in the Arabidopsis
623 phyllosphere. *Nature Ecology & Evolution* **3**: 1445–1454.
- 624 **Chavarro-Carrero EA, Vermeulen JP, Torres DE, Usami T, Schouten HJ, Bai Y, Seidl**
625 **MF, Thomma BPHJ. 2021.** Comparative genomics reveals the *in planta*-secreted *Verticillium*
626 *dahliae* Av2 effector protein recognized in tomato plants that carry the *V2* resistance locus.
627 *Environmental Microbiology* **23**: 1941–1958.
- 628 **Chen T, Nomura K, Wang X, Sohrabi R, Xu J, Yao L, Paasch BC, Ma L, Kremer J,**
629 **Cheng Y. 2020.** A plant genetic network for preventing dysbiosis in the phyllosphere. *Nature*

- 630 **580**: 653–657.
- 631 **Chisholm ST, Coaker G, Day B, Staskawicz BJ. 2006.** Host-microbe interactions: shaping
632 the evolution of the plant immune response. *Cell* **124**: 803–814.
- 633 **Conn VM, Walker AR, Franco CMM. 2008.** Endophytic actinobacteria induce defense
634 pathways in *Arabidopsis thaliana*. *Molecular Plant-Microbe Interactions* **21**: 208–218.
- 635 **Cook DE, Kramer HM, Torres DE, Seidl MF, Thomma BPHJ. 2020.** A unique chromatin
636 profile defines adaptive genomic regions in a fungal plant pathogen. *Elife* **9**: e62208.
- 637 **Cook DE, Mesarich CH, Thomma BPHJ. 2015.** Understanding plant immunity as a
638 surveillance system to detect invasion. *Annual review of phytopathology* **53**: 541–563.
- 639 **Depotter JRL, Shi-Kunne X, Missonnier H, Liu T, Faino L, van den Berg GCM, Wood
640 TA, Zhang B, Jacques A, Seidl MF. 2019.** Dynamic virulence-related regions of the plant
641 pathogenic fungus *Verticillium dahliae* display enhanced sequence conservation. *Molecular
642 ecology* **28**: 3482–3495.
- 643 **Dini-Andreote F. 2020.** Endophytes: The Second Layer of Plant Defense. *Trends in Plant
644 Science* **25**: 319–322.
- 645 **Diwan N, Fluhr R, Eshed Y, Zamir D, Tanksley SD. 1999.** Mapping of *Ve* in tomato: a gene
646 conferring resistance to the broad-spectrum pathogen, *Verticillium dahliae* race 1. *Theoretical
647 and Applied Genetics* **98**: 315–319.
- 648 **Dodds PN, Rathjen JP. 2010.** Plant immunity: towards an integrated view of plant–pathogen
649 interactions. *Nature Reviews Genetics* **11**: 539–548.
- 650 **Dong S, Raffaele S, Kamoun S. 2015.** The two-speed genomes of filamentous pathogens:
651 waltz with plants. *Current opinion in genetics & development* **35**: 57–65.
- 652 **Faino L, Seidl MF, Datema E, van den Berg GCM, Janssen A, Wittenberg AHJ, Thomma
653 BPHJ. 2015.** Single-molecule real-time sequencing combined with optical mapping yields
654 completely finished fungal genome. *MBio* **6**.

- 655 **Faino L, Seidl MF, Shi-Kunne X, Pauper M, van den Berg GCM, Wittenberg AHJ,**
656 **Thomma BPHJ. 2016.** Transposons passively and actively contribute to evolution of the two-
657 speed genome of a fungal pathogen. *Genome Research* **26**: 1091–1100.
- 658 **Fradin EF, Thomma BPHJ. 2006.** Physiology and molecular aspects of *Verticillium* wilt
659 diseases caused by *V. dahliae* and *V. albo-atrum*. *Molecular Plant Pathology* **7**: 71–86.
- 660 **Fradin EF, Zhang Z, Ayala JCJ, Castroverde CDM, Nazar RN, Robb J, Liu C-M,**
661 **Thomma BPHJ. 2009.** Genetic dissection of *Verticillium* wilt resistance mediated by tomato
662 *Ve1*. *Plant physiology* **150**: 320–332.
- 663 **Fradin EF, Zhang Z, Rovenich H, Song Y, Liebrand TWH, Masini L, van den Berg GCM,**
664 **Joosten MHAJ, Thomma BPHJ. 2014.** Functional Analysis of the Tomato Immune Receptor
665 *Ve1* through Domain Swaps with Its Non-Functional Homolog *Ve2*. *PLoS ONE* **9**: e88208.
- 666 **Frandsen RJN, Andersson JA, Kristensen MB, Giese H. 2008.** Efficient four fragment
667 cloning for the construction of vectors for targeted gene replacement in filamentous fungi.
668 *BMC Molecular Biology* **9**: 70.
- 669 **Gómez-Pérez D, Schmid M, Chaudhry V, Velic A, Maček B, Maček M, Kemen A, Kemen**
670 **E. 2022.** Proteins released into the plant apoplast by the obligate parasitic protist *Albugo*
671 selectively repress phyllosphere-associated bacteria. *bioRxiv*: 2022.05.16.492175.
- 672 **Gout L, Kuhn ML, Vincenot L, Bernard-Samain S, Cattolico L, Barbetti M, Moreno-**
673 **Rico O, Balesdent M, Rouxel T. 2007.** Genome structure impacts molecular evolution at the
674 *AvrLm1* avirulence locus of the plant pathogen *Leptosphaeria maculans*. *Environmental*
675 *Microbiology* **9**: 2978–2992.
- 676 **Hassani MA, Odiezkurt E, Seybold H, Dagan T, Stukenbrock EH. 2019.** Interactions and
677 coadaptation in plant metaorganisms. *Annual Reviews* **57**: 483–503.
- 678 **He Q, McLellan H, Boevink PC, Birch PRJ. 2020.** All roads lead to susceptibility: the many
679 modes of action of fungal and oomycete intracellular effectors. *Plant Communications* **1**:

680 100050.

681 **Jones JDG, Dangl JL. 2006.** The plant immune system. *nature* **444**: 323–329.

682 **de Jonge R, Bolton MD, Kombrink A, van den Berg GCM, Yadeta KA, Thomma BPHJ.**

683 **2013.** Extensive chromosomal reshuffling drives evolution of virulence in an asexual pathogen.

684 *Genome research* **23**: 1271–1282.

685 **de Jonge R, Peter van Esse H, Maruthachalam K, Bolton MD, Santhanam P, Saber MK,**

686 **Zhang Z, Usami T, Lievens B, Subbarao K V., et al. 2012.** Tomato immune receptor Ve1

687 recognizes effector of multiple fungal pathogens uncovered by genome and RNA sequencing.

688 *Proceedings of the National Academy of Sciences* **109**: 5110–5115.

689 **van Kan JAL, Van den Ackerveken G, De Wit P. 1991.** Cloning and characterization of

690 cDNA of avirulence gene *avr9* of the fungal pathogen *Cladosporium fulvum*, causal agent of

691 tomato leaf mold. *Mol. Plant-Microbe Interact* **4**: 52–59.

692 **Kawchuk LM, Hachey J, Lynch DR, Kulcsar F, Van Rooijen G, Waterer DR, Robertson**

693 **A, Kokko E, Byers R, Howard RJ. 2001.** Tomato *Ve* disease resistance genes encode cell

694 surface-like receptors. *Proceedings of the National Academy of Sciences* **98**: 6511–6515.

695 **Klosterman SJ, Subbarao K V, Kang S, Veronese P, Gold SE, Thomma BPHJ, Chen Z,**

696 **Henrissat B, Lee Y-H, Park J. 2011.** Comparative genomics yields insights into niche

697 adaptation of plant vascular wilt pathogens. *PLoS pathogens* **7**.

698 **Kombrink A, Rovenich H, Shi-Kunne X, Rojas-Padilla E, van den Berg GCM,**

699 **Domazakis E, De Jonge R, Valkenburg D, Sánchez-Vallet A, Seidl MF. 2017.** *Verticillium*

700 *dahliae* LysM effectors differentially contribute to virulence on plant hosts. *Molecular plant*

701 *pathology* **18**: 596–608.

702 **Langmead B, Salzberg SL. 2012.** Fast gapped-read alignment with Bowtie 2. *Nature methods*

703 **9**: 357.

704 **Lee S-M, Kong HG, Song GC, Ryu C-M. 2021.** Disruption of Firmicutes and Actinobacteria

705 abundance in tomato rhizosphere causes the incidence of bacterial wilt disease. *The ISME*
706 *journal* **15**: 330–347.

707 **Li H. 2018.** Minimap2: pairwise alignment for nucleotide sequences. *Bioinformatics* **34**: 3094–
708 3100.

709 **Li J. 2019.** Identification of host-specific effectors mediating pathogenicity of the vascular wilt
710 pathogen *Verticillium dahliae*. Wageningen University PhD thesis.

711 **Li J, Cornelissen B, Rep M. 2020.** Host-specificity factors in plant pathogenic fungi. *Fungal*
712 *Genetics and Biology* **144**: 103447.

713 **Li H, Durbin R. 2009.** Fast and accurate short read alignment with Burrows–Wheeler
714 transform. *Bioinformatics* **25**: 1754–1760.

715 **Niu X, Zhao X, Ling K-S, Levi A, Sun Y, Fan M. 2016.** The *FonSIX6* gene acts as an
716 avirulence effector in the *Fusarium oxysporum* f. sp. *niveum*-watermelon pathosystem.
717 *Scientific reports* **6**: 1–7.

718 **Praz CR, Bourras S, Zeng F, Sánchez-Martín J, Menardo F, Xue M, Yang L, Roffler S,**
719 **Böni R, Herren G. 2017.** *AvrPm2* encodes an RNase-like avirulence effector which is
720 conserved in the two different specialized forms of wheat and rye powdery mildew fungus.
721 *New Phytologist* **213**: 1301–1314.

722 **Quinlan AR, Hall IM. 2010.** BEDTools: a flexible suite of utilities for comparing genomic
723 features. *Bioinformatics* **26**: 841–842.

724 **Raffaele S, Kamoun S. 2012.** Genome evolution in filamentous plant pathogens: why bigger
725 can be better. *Nature Reviews Microbiology* **10**: 417–430.

726 **Rovenich H, Boshoven JC, Thomma BPHJ. 2014.** Filamentous pathogen effector functions:
727 of pathogens, hosts and microbiomes. *Current opinion in plant biology* **20**: 96–103.

728 **Santhanam P. 2012.** Random insertional mutagenesis in fungal genomes to identify virulence
729 factors. In: Thomma BPHJ, Bolton MD, Plant Fungal Pathogens. Springer, 509–517.

- 730 **Schaible L, Cannon OS, Waddoups V. 1951.** Inheritance of resistance to *Verticillium* wilt in
731 a tomato cross. *Phytopathology* **41**.
- 732 **Schmidt SM, Lukasiewicz J, Farrer R, van Dam P, Bertoldo C, Rep M. 2016.** Comparative
733 genomics of *Fusarium oxysporum* f. sp. *melonis* reveals the secreted protein recognized by the
734 *Fom-2* resistance gene in melon. *New Phytologist* **209**: 307–318.
- 735 **Shi-Kunne X, Faino L, van den Berg GCM, Thomma BPHJ, Seidl MF. 2018.** Evolution
736 within the fungal genus *Verticillium* is characterized by chromosomal rearrangement and gene
737 loss. *Environmental microbiology* **20**: 1362–1373.
- 738 **Snelders NC, Petti GC, van den Berg GCM, Seidl MF, Thomma BPHJ. 2021.** An ancient
739 antimicrobial protein co-opted by a fungal plant pathogen for in planta mycobiome
740 manipulation. *Proceedings of the National Academy of Sciences* **118**: e2110968118.
- 741 **Snelders NC, Rovenich H, Petti GC, Rocafort M, van den Berg GCM, Vorholt JA,
742 Mesters JR, Seidl MF, Nijland R, Thomma BPHJ. 2020.** Microbiome manipulation by a
743 soil-borne fungal plant pathogen using effector proteins. *Nature Plants* **6**: 1365–1374.
- 744 **Snelders NC, Rovenich H, Thomma BPHJ. 2022.** Microbiota manipulation through the
745 secretion of effector proteins is fundamental to the wealth of lifestyles in the fungal kingdom.
746 *FEMS Microbiology Reviews* **2022**: 1–16.
- 747 **Stamatakis A. 2014.** RAxML version 8: a tool for phylogenetic analysis and post-analysis of
748 large phylogenies. *Bioinformatics* **30**: 1312–1313.
- 749 **Stergiopoulos I, De Kock MJD, Lindhout P, De Wit PJGM. 2007.** Allelic variation in the
750 effector genes of the tomato pathogen *Cladosporium fulvum* reveals different modes of
751 adaptive evolution. *Molecular Plant-Microbe Interactions* **20**: 1271–1283.
- 752 **Thomma BPHJ, Nürnberger T, Joosten MHAJ. 2011.** Of PAMPs and effectors: the blurred
753 PTI-ETI dichotomy. *The plant cell* **23**: 4–15.
- 754 **Torres DE, Oggenfuss U, Croll D, Seidl MF. 2020.** Genome evolution in fungal plant

755 pathogens: looking beyond the two-speed genome model. *Fungal Biology Reviews* **34**: 136–
756 143.

757 **Torres DE, Thomma BPHJ, Seidl MF. 2021.** Transposable Elements Contribute to Genome
758 Dynamics and Gene Expression Variation in the Fungal Plant Pathogen *Verticillium dahliae*.
759 *Genome Biology and Evolution* **13**.

760 **Usami T, Momma N, Kikuchi S, Watanabe H, Hayashi A, Mizukawa M, Yoshino K,**
761 **Ohmori Y. 2017.** Race 2 of *Verticillium dahliae* infecting tomato in Japan can be split into two
762 races with differential pathogenicity on resistant rootstocks. *Plant Pathology* **66**: 230–238.

763 **Wang Y, Pruitt RN, Nürnberger T, Wang Y. 2022.** Evasion of plant immunity by microbial
764 pathogens. *Nature Reviews Microbiology*: 1–16.

765 **Wu W, Wang L, Zhang S, Li Z, Zhang Y, Lin F, Pan Q. 2014.** Stepwise arms race between
766 *AvrPik* and *Pik* alleles in the rice blast pathosystem. *Molecular Plant-Microbe Interactions* **27**:
767 759–769.

768 **Zhang Z, Fradin E, de Jonge R, van Esse HP, Smit P, Liu C-M, Thomma BPHJ. 2013.**
769 Optimized agroinfiltration and virus-induced gene silencing to study Ve1-mediated
770 *Verticillium* resistance in tobacco. *Molecular plant-microbe interactions* **26**: 182–190.

771 **Zhou L, Zhao J, Guo W, Zhang T. 2013.** Functional analysis of autophagy genes via
772 *Agrobacterium*-mediated transformation in the vascular wilt fungus *Verticillium dahliae*.
773 *Journal of genetics and genomics* **40**: 421–431.